Tetrahedron xxx (2015) 1–10

Contents lists available at ScienceDirect

Tetrahedron

journal homepage: www.elsevier.com/locate/tet

A family of extended heterocyclic oligomers with thienylene/thiazolylene vinylene cores and triphenylamino/carbazolyl terminals

Bin Xi, Na Wang, Bin-Bin Ma, Tao Tao, Wei Huang *

State Key Laboratory of Coordination Chemistry, Nanjing National Laboratory of Microstructures, School of Chemistry and Chemical Engineering, Nanjing University, Nanjing 210093, PR China

ARTICLE INFO

Article history:
Received 11 March 2015
Received in revised form 12 April 2015
Accepted 16 April 2015
Available online xxx

Keywords:
Thienylene vinylene compound
Thiazolylene vinylene compound
C–C and C=C bond coupling
Triphenylamino chromophore
Carbazolyl chromophore
Crystal structure

ABSTRACT

A series of semiconducting thienylene/thiazolylene vinylene oligomers with triphenylamino/carbazolyl terminal groups have been designed and prepared successfully. Synthetic, structural, thermal, spectral and electrochemical comparisons have been carried out for related compounds. The photophysical results demonstrate that all the vinylene oligomers and their precursors show high luminescence quantum yields. In addition, X-ray single-crystal structure analysis of a typical thiophene based double-bond compound **7** indicates a molecular length of 2.72 nm with the *E*-configuration.

1. Introduction

π-Conjugated polymers and oligomers have attracted tremendous attention in the field of molecular based materials[1] because of the roles they play in organic light-emitting diodes (OLEDs),[2] organic solar cells (OSCs)[3] and organic thin film transistor (OTFTs).[4] Up to date, numerous studies on oligo- and polythiophenes have been carried out. These materials have good chemical stability in both oxidized and reduced forms, and diverse functionality can be readily built-in.[5] Particularly, oligothiophenes are the most versatile and effective molecular scaffolds for organic functional materials[6] with significantly improved optical and electronic properties.[7] However, a detailed understanding of the relationship between the electronic structure, crystal packing, and device performance is still a significant challenge.[8]

Different coupling reactions such as Suzuki, Stille, Negeshi and Kumada reactions, have been widely used for the aromatic heterocyclic extension. However, these reactions will encounter the conflicts between introducing long alkyl chains to improve the solubility of target molecules and maintaining molecular planarity to ensure good π-conjugated system. In contrast, using extended double bond bridges by McMurry reaction to link adjacent aromatic heterocycles in the absence of long alkyl chains is an effective approach to solve the solubility problem. Meanwhile, introduction of the C=C unit could maintain the planarity[9] and the effective conjugated system of the whole molecules.[10,11] However, McMurry reaction is a little more difficult to operate because of the lower reaction activities of Ti(IV) than Pd(0) catalysts.

Thienylene vinylene core is often used for preparing oligomers and polymers in the field of photoelectric materials.[12,13] However, investigations have seldom been carried out on thiazolylene vinylene based aromatic heterocyclic compounds yet. The combination of thienylene/thiazolylene vinylene cores and triphenylamino/carbazolyl terminals has not been explored. In our previous work, a series of oligothiophene and thiazole/bithiazole based heterocyclic aromatic compounds with different terminal chromophores have been described.[14] In the current study, we intend to prepare a new family of semiconducting oligomers composed of thienylene/thiazolylene vinylene cores and triphenylamino/carbazolyl terminals (Scheme 1), and compare the corresponding synthetic, structural, spectral, electrochemical and DFT computational results. Herein, eight new compounds including three precursors and one by-product from McMurry reaction, are reported. Among them, two pairs of thienylene/thiazolylene vinylene semiconducting compounds with two triphenylamino/4-(9*H*-carbozol-

* Corresponding author. E-mail address: whuang@nju.edu.cn (W. Huang).

http://dx.doi.org/10.1016/j.tet.2015.04.045
0040-4020/

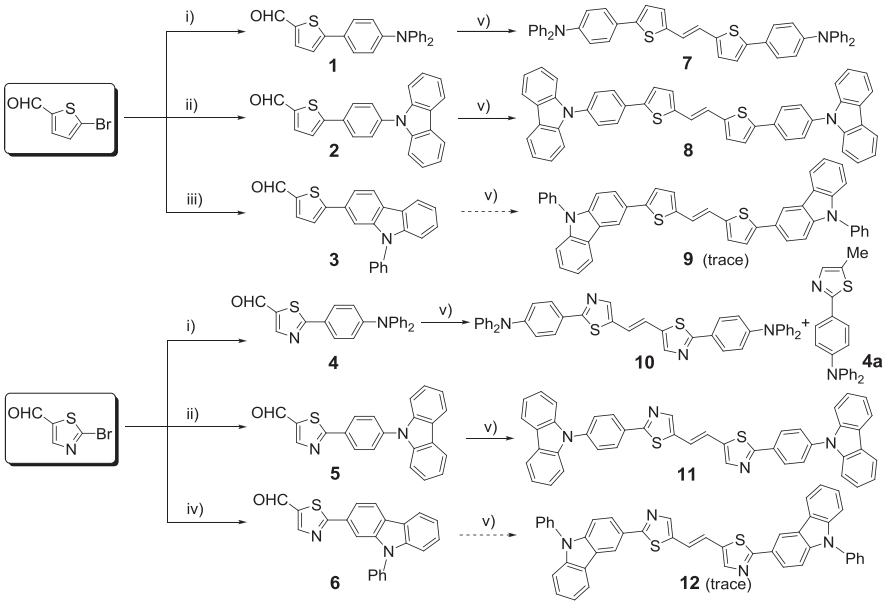

Scheme 1. Synthetic route for the thiophene and thiazole based aromatic heterocyclic fluorescent compounds extended by triphenylamino and carbazolyl chromophores.

9-yl)phenyl terminal groups have been focused. In addition, X-ray single-crystal structure of one typical thiophene based double-bond compound **7** shows the *E*-configuration with a molecular length of 2.72 nm.

2. Results and discussion

2.1. Syntheses and spectral characterizations

Our synthetic strategy herein is based on the combination of C–C single bond Suzuki-Miyaura cross-coupling and C=C double bond McMurry reaction from 5-bromothiophene-2-carbaldehyde and 2-bromothiazole-5-carbaldehyde to build extended aromatic heterocycles. However, it is found that the sequence of two cross-coupling reactions is very important in our experiments, especially for thiazole based compounds because of the relatively lower electron density of thiazole ring. One control experiment revealed no product for McMurry reaction from 2-bromothiazole-5-carbaldehyde precursor, so Suzuki-Miyaura cross-coupling reaction was firstly selected to prepare thiophene and thiazole based aldehyde precursors **1**–**6** because introduction of the electron-donating triphenylamino/carbazolyl chromophores could effectively improve the reaction activities for the next McMurry reaction. As a result, two pairs of triphenylamine (TPA) and 4-(9*H*-carbozol-9-yl)phenyl terminated thienylene and thiazolylene vinylene extended aromatic heterocyclic compounds (**7**, **8**, **10** and **11**) have been successfully yielded. In addition, thiophene involved couplings had much higher reaction activities and yields than the thiazole based ones in our experiments owing to the presence of more electron-rich thiophene ring.

Reductive McMurry coupling of aldehydes **1** and **2** afforded thienylene vinylene oligomers **7** and **8** in the yields of 52 and 47%, while the yields for compounds **10** and **11** were calculated to be 45 and 31%. In addition, a reduced compound **4a** was separated successfully with a 10% yield during the preparation of compound **10**. It should be mentioned that attempts for separating compounds **9** and **12** via similar McMurry reaction from compounds **3** and **6** having isomeric 9-phenyl-9*H*-carbazol-3-yl moiety were not successful, where only traced products could be detected with very close R_f values (Fig. 1). We think the possible reason may be the relatively low reaction activity of 4-(9*H*-carbozol-9-yl)phenylboronic acid in comparison with 4-(diphenylamino)phenylboronic acid, which led to complicated products and low yields in both Suzuki and McMurry couplings. In this case, purification of compounds **9** and **12** to give available ^{1}H NMR spectra was not successful. However, the existence of **9** and **12** could be verified by EI–TOF–MS analysis as well as comparing TLC plates with **7**, **8**, **10** and **11** (Figs. SD9 and 10).

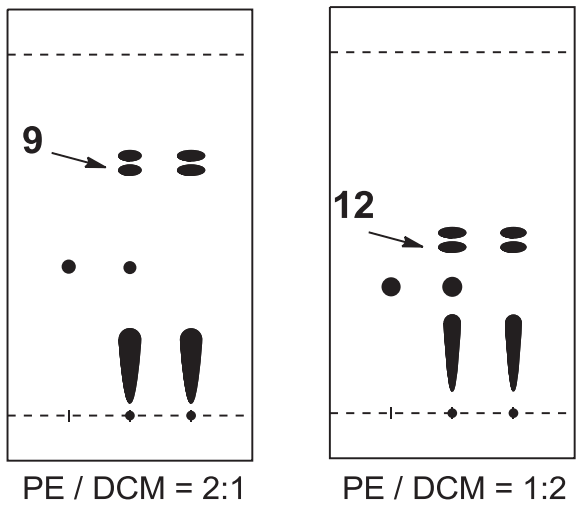

Fig. 1. TLC plates of McMurry reaction for preparing compounds **9** and **12**.

All the heterocyclic aromatic compounds have been characterized by ^{1}H, ^{13}C NMR and EI–TOF–MS spectra, and the results clearly

demonstrate the formation of expected molecules. Single-crystal structure of thienylene vinylene oligomer **7** displays the double-bond oligomers as *E*-configuration and has reached a molecular length of 2.72 nm. All the thiophene and thiazole based vinylene oligomers (**7**, **8**, **10** and **11**) exhibit good thermal stabilities with the Td_{10} (10% weight-loss temperature) values higher than 300 °C in their thermogravimetric analysis (TGA), as displayed in Fig. SD11. Our experimental results in this work indicate that the thermal behavior of these vinylene oligomers is comparable with our previously reported single-bond linked thiazole based compounds **19** and **20**.[14b] In addition, thiazole based vinylene oligomers possess better thermal stability in comparison with thiophene based ones, whilst the triphenylamine terminated compounds exhibits better thermal stability than corresponding 4-(9*H*-carbozol-9-yl)phenyl terminated ones. The discrepancy of thermal stability is suggested to be their different molecular polarity, molecular weight and corresponding van der Waals' force.

All thiophene and thiazole based heterocyclic aromatic compounds show characteristic absorptions at 360–444 nm in their electronic spectra ascribed to the π–π* transitions between substituted heterocycles in different π-conjugated system (Fig. 2a and b). With the extension of conjugation lengths, significant bathochromic shifts on maximum absorption wavelengths (λ_{max}) have been observed from aldehyde precursors **1**–**6** (λ_{max}=360–418 nm) to oligomers **7**, **8**, **10** and **11** (λ_{max}=417–444 nm) after McMurry reaction. Owing to efficient intramolecular charge transfer caused by large π-conjugated system, thiazole based precursors **4**–**6** (λ_{max}=376–418 nm) exhibit bathochromic shifts in contrast to thiophene based derivatives **1**–**3** (λ_{max}=360–408 nm). Furthermore, solid state UV–vis absorption experiments have been carried out for compounds **7**, **8**, **10** and **11** (Fig. SD12). It is found that thiophene based derivatives (**7** and **10**) also display bathochromic shifts in comparison with thiazole based ones (**8** and **11**), which is analogous to their behavior in solution.

In order to give a better understanding of the thienylene/thiazolylene vinylene oligomers, molecular structures and λ_{max} values of some previously reported compounds **13**–**17**[15] with the same thienylene vinylene core as well as single-bond linked thienyl and thiazolyl heterocycles **18**–**20**[14b] are listed in Scheme 2 and Table 1 for comparison. Remarkable bathochromic shifts are found in comparison with compounds **13** and **14** with shorter π-conjugated system, while similar λ_{max} values can be observed for compounds **15** and **17** having thienylene vinylene core. However, the λ_{max} value of compound **16** (388 nm) with two naphthyl terminal groups shows a less bathochromic shift, in comparison with the electron-donating thienyl, triphenylamino and carbazolyl terminals. Furthermore, compounds **7**, **8**, **10** and **11** in this work have comparable λ_{max} values with our previously reported TPA-terminated oligomers **18**–**20** with single-bond linked thienyl and thiazolyl heterocycles.

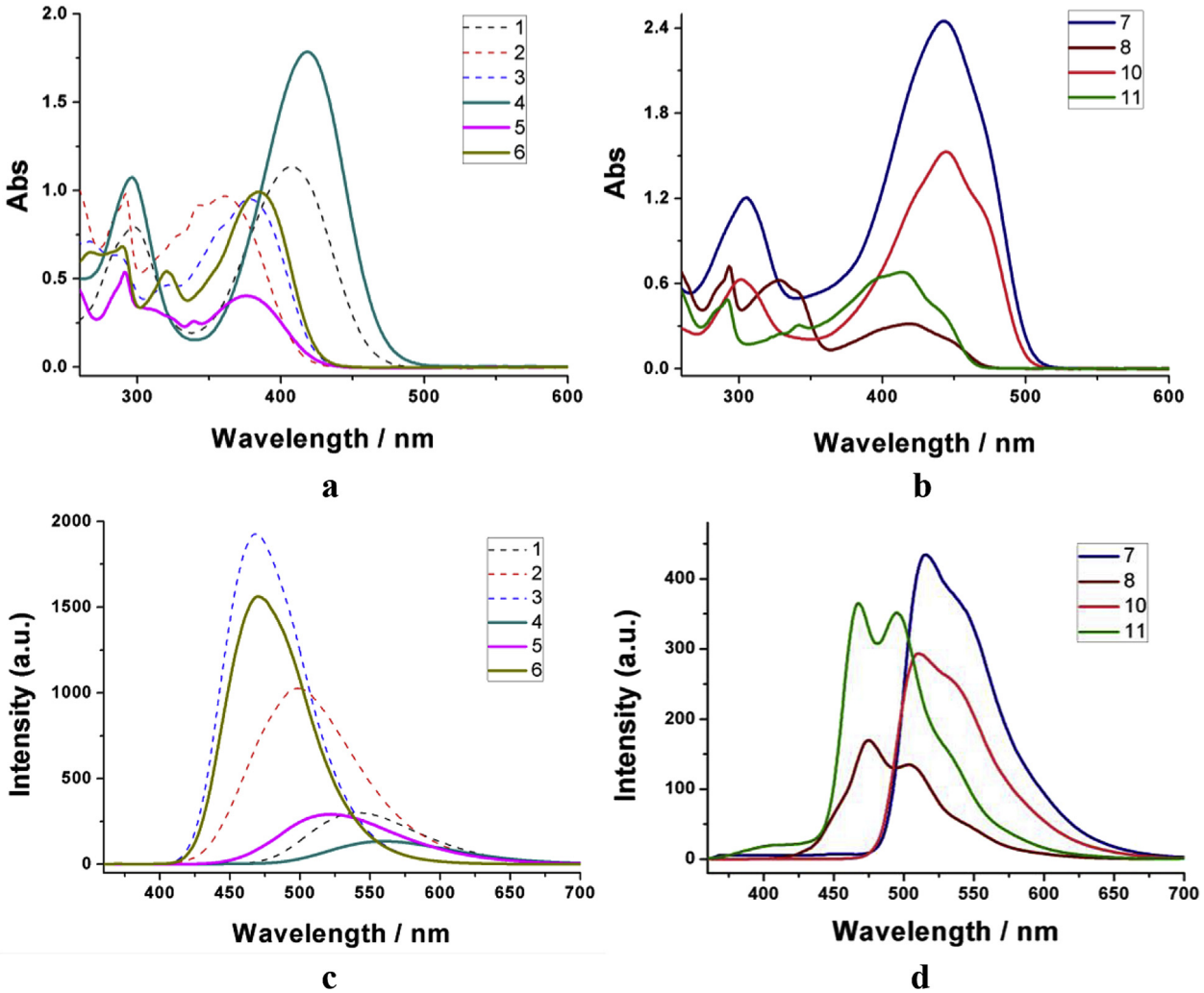

Fig. 2. UV–vis absorption spectra (a and b) and fluorescence emission spectra excited at 350 nm (c and d) for the heterocyclic aromatic compounds in their CH_2Cl_2 solutions at room temperature with the same concentration of 5.0×10^{-5} mol L^{-1}. Previously reported compounds **1**–**3** are represented as dotted lines for comparison.

Please cite this article in press as: Xi, B.; et al., Tetrahedron (2015), http://dx.doi.org/10.1016/j.tet.2015.04.045

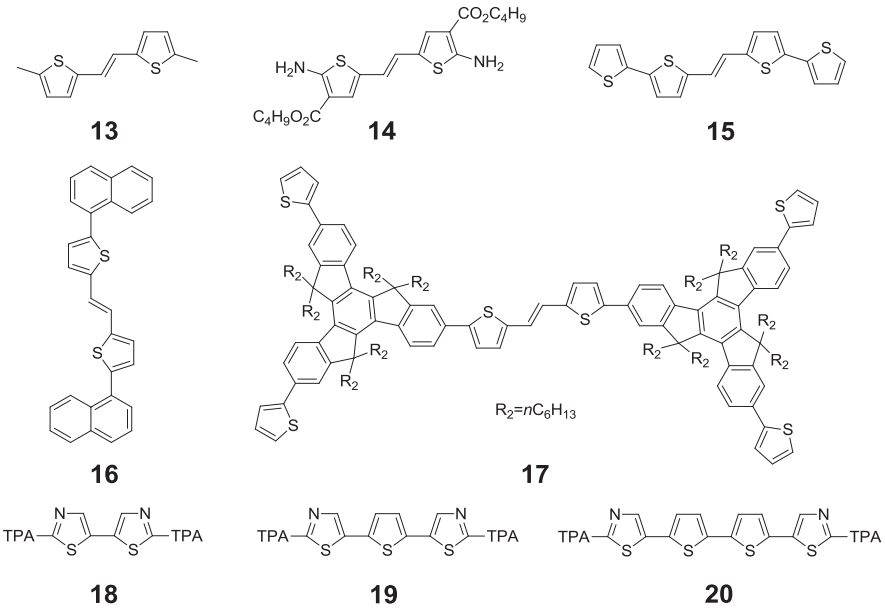

Scheme 2. Analogous compounds reported in literature for comparisons with oligomers **7**, **8**, **10** and **11**.

Table 1
UV–vis absorption and fluorescence emission data, optical, electrochemistry and calculated HOMO-LUMO energy gaps (*Eg*) for related heterocyclic aromatic compounds

Compound	UV–vis λ_{max} [nm (eV)]	ε (L mol^{-1} cm^{-1})	Eg^{opt} [a] (eV)	Eg^{calcd} [b] (eV)	Fluorescence		Td_{10} [d] (°C)	E_{ox}^{onset} [e] (V)	E_{HOMO} [f] (eV)	E_{LUMO} [g] (eV)
					λ_{max} (nm)	Φ_s [c]				
7	443 (2.80)	49,000	2.46	2.78	515	0.42	309	0.53, 0.79	−5.63	−3.17
8	417 (2.97)	6400	2.63	2.75	475	0.20	296	0.60, 0.82	−5.70	−3.07
10	444 (2.79)	30,600	2.49	2.73	510	0.34	314	0.76, 1.05	−5.86	−3.37
11	418 (2.97)	11,200	2.68	2.74	468	0.37	303	0.66, 1.02	−5.76	−3.08
13[15a]	353 (3.52)				412	0.05				
14[15a]	382 (3.25)				500	0.07				
15[15b]	422 (2.94)				448					
16[15c]	388 (3.20)	40,300			475	0.19				
17[15d]	442 (2.81)	110,000			495	0.56				
18[14b]	422 (2.94)	15,500	2.53	2.93	510	0.20	503	0.33	−5.43	−2.90
19[14b]	421 (2.94)	25,800	2.50	2.75	503	0.16	323	0.25	−5.35	−2.85
20[14b]	425 (2.92)	46,500	2.47	2.64	509	0.16	318	0.34	−5.44	−2.97

[a] Optical energy gaps determined from the UV–vis absorptions in their dichloromethane solutions.
[b] The geometries are calculated by B3LYP method and 6-31G* basis set.
[c] Photoluminescence quantum yields.
[d] 10% Weight-loss temperature.
[e] Oxidation onset potentials determined from DPV.
[f] Calculated from $E_{HOMO}=-(E_{ox}^{onset}+5.10)$.
[g] Calculated from $E_{LUMO}=E_{HOMO}+Eg^{opt}$.

Moreover, fluorescence emission spectral studies demonstrate that all six precursors (Fig. 2c) and four vinylene oligomers (Fig. 2d) are fluorescent active because of their D-π-A and D-π-π-D structures. Similar to their UV–vis spectra, triphenylamine terminated oligomers (**7** and **10**) illustrate significant bathochromic shifts of 40 and 42 nm (Table 1) compared with corresponding carbazole terminated ones (**8** and **11**). Further experiments on luminescence quantum yields (Φ_s) reveal that triphenylamine extended compound **7** has a remarkable Φ_s value of 0.42, which is the highest one among four thienylene/thiazolylene vinylene oligomers.

2.2. Electrochemical properties

The electrochemical behavior of the target compounds was examined by cyclic voltammetry (CV) and differential pulse voltammetry (DPV) measures in their 1.0×10^{-3} M solutions in dichloromethane containing 0.1 M $TBAClO_4$ as the supporting electrolyte in Fig. 3. All potentials reported herein were calibrated with the ferrocene/ferrocenium couple (Fc/Fc^+) as the internal standard. Oxidation onset potentials (E_{ox}^{onset}), as well as HOMO/LUMO energy levels determined by a combined analysis of the CV, DPV and absorption spectral data are summarized in Table 1. The onset oxidation was measured relative to the Fc/Fc^+ couple for which an energy level of −5.10 eV versus vacuum was assumed.[16]

As depicted in Fig. 3a, thienylene vinylene oligomer **7** shows reversible redox response at different scanning rates. In contrast, oligomers **8** and **10** (Fig. 3b and c) exhibit only quasi-reversible oxidation and reduction processes in the parallel experiments. The reason may be the electrochemical polymerization of thiophene and thiazole units, which will interfere with the redox response in the CV measurements. Instead, the DPV method is used to further explore the electrochemical properties of two pairs of thienylene/thiazolylene vinylene centered compounds. As can be seen in Fig. 3d, two oxidation waves are observed for all compounds, and the oxidation potentials as well as the measured currents are found to be dependent on their molecular structures. The

Please cite this article in press as: Xi, B.; et al., Tetrahedron (2015), http://dx.doi.org/10.1016/j.tet.2015.04.045

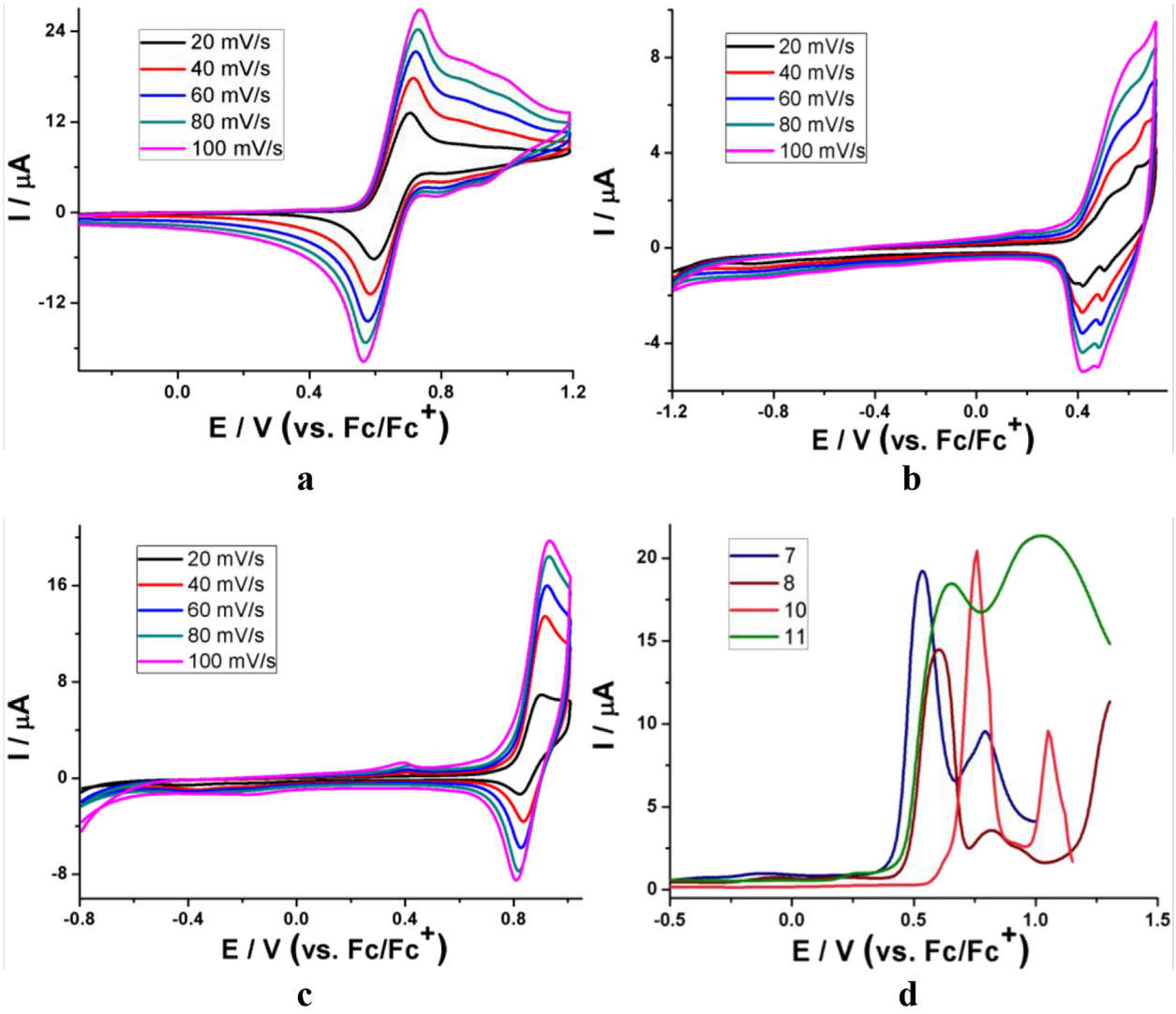

Fig. 3. CV (a, b, c) and DPV (d) for heterocyclic aromatic compounds in CH_2Cl_2 (1.0×10^{-3} M) containing 0.10 M of $TBAClO_4$ under argon. The different scanning rate: 20, 40, 60, 80, 100 mV/s (a) **7**; (b) **8**; (c) **10** versus Fc/Fc^+.

first oxidation wave can be attributed to the formation of cation-radical species and the second one is ascribed to the successive oxidation of cation-radical to its corresponding dication, which are comparable with our previously reported single-bond linked thienyl and thiazolyl heterocyclic compounds.[14b] The first E_{ox}^{onset} of these compounds in their DPV curves are determined to be 0.53 V for **7**, 0.60 V for **8**, 0.76 V for **10**, and 0.66 V for **11**, which indicates that thiophene based vinylene oligomers possess lower HOMO levels for better hole transport. In addition, density function theory (DFT) computations have been carried out to compare the energy levels of our compounds as shown in Fig. SD13, and the results are consistent with measured UV–vis absorption and electrochemical spectral data as well as previously reported oligothiophene and oligothiazole compounds.

2.3. Single-crystal structures

In this work, we have obtained five single-crystal structures (Table 2) to fully characterize their molecular geometry and further illuminate and compare their packing modes and supramolecular interactions. As can be seen, the thiophene/thiazole rings and their adjacent heterocyclic substituents in all five compounds adopt the same *trans* configuration. However, the dihedral angles between them are different, as depicted in Fig. 4a. The dihedral angles between the thiophene/thiazole rings and adjacent aromatic units in compounds **2**, **4**, **4a** and **6** are calculated to be 5.3(1)–21.9(2)°. In contrast, the dihedral angles between benzene and carbazole rings in the *N*-phenylcarbazole unit in compounds **2** and **6** are much larger at 50.9(2) and 59.0(1)°, respectively. In triphenylamine terminated thienylene vinylene compound **7**, the molecular length reaches to 2.72 nm, where the middle two thiophene rings at each side of double bond are essentially coplanar with the dihedral angles of 6.3(2) and 12.5(3)°.

π–π Stacking interactions are found in the cases of compounds **4**, **6** and **7**. One thiazole ring in **4** is packed with its neighboring counterpart with the centroid-to-centroid separation of 3.979(2) Å, and the centroid-to-centroid separations between neighboring heterocyclic aromatic rings in **6** are found to be 3.689(2), 3.502(2) and 3.938(1) Å. In contrast, a dimeric packing mode is observed in **7** where the π–π stacking interactions between adjacent thiophene rings are found to be 3.803(5) Å (Fig. 4b).

2.4. Semiconducting properties

Temperature-dependent *I*–*V* curves have been recorded for triphenylamine terminated thienylene vinylene oligomer **7** in order

Table 2
Crystal data and structure refinements for five compounds **2**, **4**, **4a**, **6** and **7**

Compound	**2**	**4**	**4a**	**6**	**7**
Formula	$C_{23}H_{15}NOS$	$C_{22}H_{16}N_2OS$	$C_{22}H_{18}N_2S$	$C_{22}H_{14}N_2OS$	$C_{46}H_{34}N_2S_2$
Formula weight	353.42	356.43	342.44	354.41	678.87
T (K)	291(2)	291(2)	291(2)	291(2)	291(2)
Wavelength (Å)	0.71073	0.71073	0.71073	0.71073	0.71073
Crystal size (mm)	0.10×0.10×0.12	0.10×0.12×0.14	0.10×0.12×0.12	0.10×0.10×0.14	0.10×0.10×0.12
Crystal system	Monoclinic	Monoclinic	Monoclinic	Monoclinic	Triclinic
Space group	$P2_1/c$	$C2/c$	$P2_1/c$	$P2_1/n$	$P\bar{1}$
a (Å)	8.001(1)	25.266(5)	14.499(1)	8.506(2)	10.265(2)
b (Å)	27.025(3)	9.877(2)	11.636(1)	7.005(1)	13.271(2)
c (Å)	8.247(1)	18.464(3)	11.226(1)	29.677(6)	13.542(2)
α (deg)	90.00	90.00	90.00	90.00	100.730(2)
β (deg)	97.133(2)	127.997(5)	109.791(2)	94.145(4)	95.538(3)
γ (deg)	90.00	90.00	90.00	90.00	101.685(3)
V (Å^3)	1769.5(4)	3631.0(11)	1782.0(3)	1763.9(6)	1757.5(5)
Z/D_{calcd} (g/cm^3)	4/1.327	8/1.304	4/1.276	4/1.335	2/1.283
F (000)	736	1488	720	736	712
μ (mm^{-1})	0.194	0.191	0.188	0.196	0.188
h_{min}/h_{max}	−10/8	−32/32	−18/17	−11/9	−7/12
k_{min}/k_{max}	−35/35	−12/12	−14/15	−8/9	−15/15
l_{min}/l_{max}	−10/10	−19/23	−14/14	−37/38	−16/16
Data/parameter	4067/235	4045/235	4117/227	4032/245	6062/451
Final R indices [$I>2\sigma(I)$ [a]]	R_1=0.0615	R_1=0.0454	R_1=0.0499	R_1=0.0400	R_1=0.0939
	wR_2=0.1475	wR_2=0.1183	wR_2=0.1393	wR_2=0.1071	wR_2=0.1903
R indices (all data [a])	R_1=0.0855	R_1=0.0675	R_1=0.0724	R_1=0.0530	R_1=0.1449
	wR_2=0.1590	wR_2=0.1320	wR_2=0.1548	wR_2=0.1150	wR_2=0.2447
S	1.089	1.031	1.069	1.044	0.980
Max./min. $\Delta\rho$ (e·Å^{-3})	0.211/−0.230	0.238/−0.368	0.361/−0.346	0.223/−0.231	0.713/−0.368

[a] $R_1=\Sigma||Fo|-|Fc||/\Sigma|Fo|$, $wR_2=[\Sigma[w(Fo^2-Fc^2)^2]/\Sigma w(Fo^2)^2]^{1/2}$.

to further verify the semiconducting property of this thiophene based compound. As can be seen in Fig. 5, ten quasi-linear I–V curves have been recorded in the temperature range 155–200 °C, and one can see that the conductance of **7** increases with the increase of temperature, indicative of typical temperature dependent semiconducting properties. It is noted that the current increases up to *ca.* 0.37 μA at 9 V when the temperature increases to 200 °C. The linear fitting of I–V curves of thienylene vinylene oligomer **7** at different temperature indicates 23 times enhancement of average conductance from 155 to 200 °C, which can be calculated from the ratio of slope between two linear fitting curves. Further Arrhenius plot [ln(T) versus 1/T][17] based on Eq. 1 reveals good linearity in the temperature range 155–200 °C at different voltage, which means that the semiconducting characteristic of **7** is governed by thermal conduction mechanism. The subsequent linear fitting of Arrhenius plot at different voltage gives the mean activation energy (ΔE) of 1.13 eV. Similarly, the linear fitting of I–V curves of thienylene vinylene compound **7** at 200 °C indicates approximate 8 times' enhancement than corresponding thiazolylene vinylene compound **10** (Fig. SD14). The average conductance increases from 1.39×10^{-5} S m^{-1} to 1.08×10^{-4} S m^{-1}, indicating that the thiophene based vinylene oligomer performs a better hole transport ability than corresponding thiazole based one.

$$I \propto \exp\left[\frac{-\Delta E}{kBT}\right] \quad (1)$$

3. Conclusion

As aromatic heterocyclic extended reactions, both Suzuki and McMurry coupling reactions have merits and shortcomings. On the one hand, Suzuki coupling offers a general method for the conversion from C–X (X=halogen atoms) to C–C single bond, while McMurry reaction provides an effective way to transform C=O into C=C double bond in aromatic heterocyclic extension. On the other hand, the former comes across the problems of solubility limitation and maintenance of the planarity of the whole molecules, while the latter meets the conflicts of operation difficulties and low yields. In this work, we have demonstrated that the synthetic strategy of combing C–C single bond and C=C double bond can be achieved, but the sequence of Suzuki and McMurry coupling reactions is very important because of the low reaction activities of thiazole unit, namely Suzuki reaction adopted first and McMurry coupling the next.

Based on the above-mentioned considerations, a family of aromatic heterocyclic extended oligomers with thienylene/thiazolylene vinylene cores and triphenylamino/carbazolyl terminals have been successfully synthesized, including two pairs of thienylene/thiazolylene vinylene centered compounds with two triphenylamino/4-(9*H*-carbozol-9-yl)phenyl terminal groups, three aldehyde precursors and one by-product. A typical triphenylamine terminated thienylene vinylene compound **7** with a molecule length of 2.72 nm has been further characterized by X-ray single-crystal diffraction. In addition, they are found to be fluorescent active with good thermal stability. All these compounds show good solubility and planarity as expected, and the thienylene vinylene oligomers display higher reaction activities and better solid-state conductance than thiazolylene vinylene ones. Further investigations are being underway in our lab on the combination of C–C single bond and C=C double bond via Suzuki and Wittig reactions, in order to achieve similar aromatic heterocyclic extensions in the applications for optoelectronic functional materials.

4. Experimental section

4.1. Materials and measurements

Solvents and reagents of analytical grade were purchased from commercial sources and used as received unless otherwise specified. THF was distilled under normal pressure from lithium aluminum hydride and benzophenone immediately prior to use. Anhydrous solvents were drawn into syringes under the flow of dry argon gas and directly transferred into the reaction flasks to avoid

Please cite this article in press as: Xi, B.; et al., Tetrahedron (2015), http://dx.doi.org/10.1016/j.tet.2015.04.045

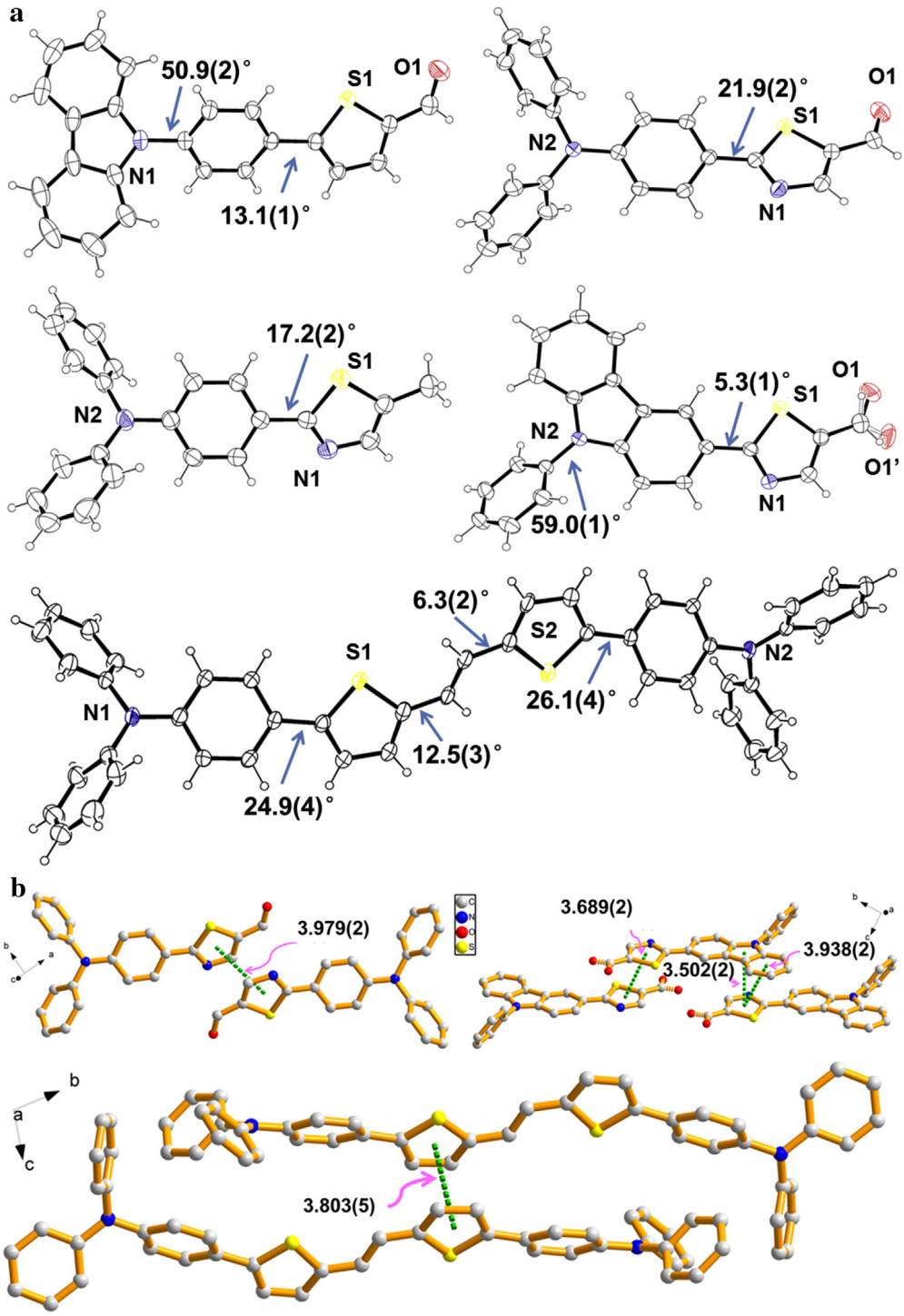

Fig. 4. a. ORTEP diagrams (30% thermal probability ellipsoids) of the molecular structures of compounds **2**, **4**, **4a**, **6** and **7** showing the dihedral angles between adjacent aromatic heterocycles. b. Perspective view of the packing structures in compounds **4**, **6** and **7** showing $\pi-\pi$ stacking interactions.

contamination. Column chromatography was carried out on silica gel (200–300 mesh) and analytical thin-layer chromatography (TLC) was performed on glass plates of silica gel GF-254 with detection by UV. Standard techniques for synthesis were carried out under argon atmosphere. Thiophene based precursors **1**–**3** were synthesized from 5-bromothiophene-2-carbaldehyde and corresponding boronic acids with high yields according to the previously reported approaches.[18] All melting points determinations were taken on a Melt-Temp apparatus and were uncorrected. Infrared (IR) spectra (4000–400 cm^{-1}) were recorded using a Nicolet FTIR 170X spectrophotometer on KBr disks. ^{1}H and ^{13}C NMR spectra were obtained on a Bruker AM-300 NMR spectrometer using TMS ($SiMe_4$) as an internal reference at room temperature. Coupling constants are given in hertz. Electroionization time-of-flight mass spectra (EI–TOF–MS, electron energy 70 eV) were recorded by mass spectrometer. Elemental analyses (EA) for carbon, hydrogen and nitrogen were performed on a Perkin–Elmer 1400C analyzer. Luminescence spectra were recorded on an F-4600 fluorescence spectrophotometer at room temperature. Thermogravimetry analyses were carried out by a NETZSCH STA449C thermogravimetric

Please cite this article in press as: Xi, B.; et al., Tetrahedron (2015), http://dx.doi.org/10.1016/j.tet.2015.04.045

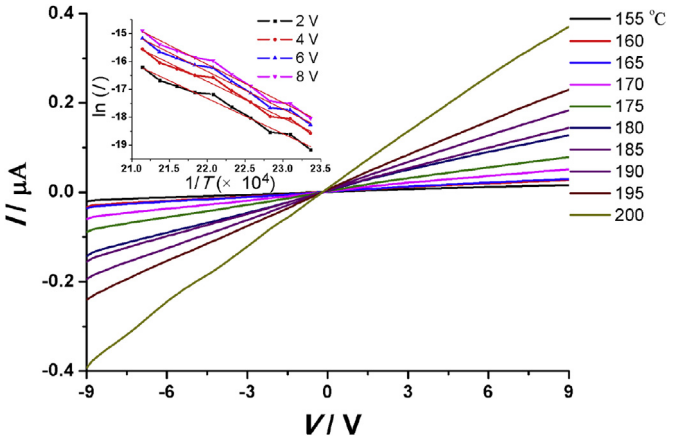

Fig. 5. Temperature-dependent *I*–*V* characteristics (155–200 °C) of compound **7** in the range −9to9 V.

analyzer in the nitrogen flow from 30 to 800 °C at a heating rate of 10.0 °C/min. UV–vis spectra were recorded with a Shimadzu UV-3150 double-beam spectrophotometer using a quartz glass cell with a path length of 10 mm.

Cyclic and differential-pulse voltammetry were performed with a CHI660D instrument, using a Pt disk as working electrode, platinum wire as the auxiliary electrode with porous ceramic wick, Ag/Ag^+ as the reference electrode, standardized for the redox couple ferrocene/ferricinium. A piece of perforated (Φ=0.1 cm) glass in the thickness of 0.2 cm was put between two ITO glass plates with a dimension of 3.0×1.0 cm^2, where each conductive ITO layer was placed in the inner side as the working electrode for the temperature-dependent *I*–*V* determination. The hole was filled with compounds **7** and **10**, respectively, in the molten state with the help of a hot plate, and the above-mentioned three glass plates were fixed together and cooled to room temperature to make sure the effective contact. *I*–*V* curves were measured by using a computer-controlled Keithley 2400 source meter.

The fluorescence quantum yield gives the efficiency of the fluorescence process, and the popular method to calculate it is to compare the fluorescence intensities (integrated areas) of a standard sample and the unknown one using the following equation.

$$\Phi_s = \Phi_{std}\left(\frac{I_s}{I_{std}}\right)\left(\frac{A_{std}}{A_s}\right)\left(\frac{\eta_s}{\eta_{std}}\right)$$

Here Φ_s is the luminescence quantum yield of the unknown sample, Φ_{std} is the luminescence quantum yield of the standard substance, *I* is the wavelength-integrated area of the corrected emission spectrum, and *A* is the absorbance value at the excitation wavelength. The η_s and η_{std} terms represent the refractive indices of the corresponding solvents (pure solvents were assumed). We use anthracene in its ethanol solution as a standard sample (Φ_{std}=0.27, η_{std}=1.36), and target compounds were dissolved in CH_2Cl_2 (η_s=1.42).[19]

DFT theoretical calculations have been made to reveal the differences between the thiazole based vinylene derivatives and corresponding thiophene based counterparts. All the DFT calculations were carried out with the Gaussian 09, revision C.01 program,[20] using the B3LYP method and 6-31G* basis set. The fixed atom coordinates of five thienyl/thiazolyl derivatives, which are based upon the structural parameters determined by the X-ray single-crystal diffraction method and the full optimization, are used for the HOMO and LUMO gap calculations (Table 1).

Single-crystal samples of compounds **2**, **4**, **4a**, **6** and **7** were covered with glue and mounted on glass fiber and then used for data collection. Crystallographic data were collected on a Bruker SMART 1K CCD diffractometer, using graphite monochromated Mo Kα radiation (λ=0.71073 Å). The crystal system was determined by Laue symmetry and the space group was assigned on the basis of systematic absences using XPREP.[21] Absorption correction was performed to the data and the structure was solved by direct methods and refined by full-matrix least-squares method on F_{obs}^2 by using the SHELXTL-PC software package.[22] All non-H atoms were anisotropically refined and all hydrogen atoms were inserted in the calculated positions assigned fixed isotropic thermal parameters and allowed to ride on their respective parent atoms. The summary of the crystal data, experimental details and refinement results for these compounds is listed in Table 2.

4.2. Syntheses and characterizations of heterocyclic aromatic compounds 4–8 and 10–11

4.2.1. Compound ***4***. Under argon atmosphere, a mixture of 2-bromothiazole-5-carbaldehyde (0.39 g, 2.00 mmol), 4-(diphenylamino)phenylboronic acid (0.87 g, 3.00 mmol), $[Pd(PPh_3)_4]$ (0.12 g, 0.10 mmol), cesium carbonate (1.95 g, 6.00 mmol), dioxane (40 mL) and deionized water (4 mL) was degassed for 10 min and heated to reflux for 24 h. The mixture was then cooled to the room temperature and extracted with chloroform. The resulting organic layer was washed thoroughly by brine and then dried with anhydrous Na_2SO_4 and filtered. After purified by column chromatography over silica gel using hexane and dichloromethane (*v*/*v*=1:2), compound **4** was obtained in a yield of 0.62 g (87%) as orange solid. Mp: 128–130 °C. Main FTIR absorptions (KBr pellets, cm^{-1}): 3440 (m), 3070 (w), 2815 (w), 1668 (s), 1585 (s), 1487 (m), 1406 (s), 1329 (s), 1223 (m), 1149 (s), 837 (m), 760 (w), 698 (m), 639 (w), 537 (w), 499 (w). ^1H NMR (300 MHz, $CDCl_3$) δ: 10.00 (s, 1H), 8.36 (s, 1H), 7.87–7.82 (dt, *J*=9.0 Hz, 2.7 Hz, 2H), 7.35–7.30 (m, 4H), 7.18–7.11 (m, 6H), 7.07–7.03 (dt, *J*=9.0 Hz, 2.7 Hz, 2H). ^{13}C NMR (75 MHz, $CDCl_3$) δ: 181.9, 175.5, 152.6, 151.2, 146.4, 137.6, 129.5, 128.3, 125.7, 125.0, 124.5, 120.8. EI–TOF–MS (*m*/*z*): calcd for $[C_{22}H_{16}N_2OS]^+$ 356.1 (100%), 357.1 (25.6%), 358.1 (4.5%), found 355.8 (100%), 354.8 (63.9%), 356.8 (7.8%). Anal. Calcd for $C_{22}H_{16}N_2OS$: C, 74.13, H, 4.52, N, 7.86%. Found: C, 74.25, H, 4.78, N, 7.90%.

4.2.2. Compound ***5***. Synthesis of this compound was similar to that described for compound **4** except that 4-(9*H*-carbozol-9-yl)phenylboronic acid (0.87 g, 3.00 mmol) was used instead of 4-(diphenylamino)phenylboronic acid. Product **5** was obtained as dark yellow solid in a yield of 0.52 g (73%). Mp: 155–157 °C. Main FTIR absorptions (KBr pellets, cm^{-1}): 3448 (m), 3058 (w), 2923 (m), 2849 (w), 1672 (s), 1600 (m), 1518 (w), 1450 (s), 1226 (s), 1161 (m), 1110 (w), 907 (w), 836 (w), 726 (m), 644 (w), 488 (w). ^1H NMR (300 MHz, $CDCl_3$) δ: 10.10 (s, 1H), 8.50 (s, 1H), 8.30–8.27 (dt, *J*=5.1 Hz, 1.2 Hz, 2H), 8.16–8.15 (d, *J*=4.8 Hz, 2H), 7.76–7.74 (dt, *J*=5.1 Hz, 1.2 Hz, 2H), 7.51–7.50 (d, *J*=4.8 Hz, 2H), 7.46–7.43 (m, 2H), 7.34–7.31 (m, 2H). ^{13}C NMR (75 MHz, $CDCl_3$) δ: 182.0, 174.3, 152.3, 140.9, 140.1, 139.1, 131.1, 128.8, 127.2, 126.2, 123.7, 120.5, 120.4, 109.7. EI–TOF–MS (*m*/*z*): calcd for $[C_{22}H_{14}N_2OS]^+$ 354.1 (100%), 355.1 (24.0%), 356.1 (4.7%), found 354.1 (100%), 355.1 (8.4%), 356.1 (0.4%). Anal. Calcd for $C_{22}H_{14}N_2OS$: C, 74.55, H, 3.98, N, 7.90%. Found: C, 74.38, H, 4.17, N, 7.99%.

4.2.3. Compound ***6***. Synthesis of this compound was similar to that described for compound **4** except that (9-phenyl-9*H*-carbazol-3-yl) boronic acid (0.87 g, 3.00 mmol) was used instead of 4-(diphenylamino)phenylboronic acid. Product **6** was obtained as dark yellow solid in a yield of 0.40 g (57%). Mp: 171–174 °C. Main FTIR absorptions (KBr pellets, cm^{-1}): 3450 (m), 2922 (m), 2852 (w), 2719 (w), 1672 (s), 1592 (m), 1499 (m), 1383 (s), 1230 (m), 1165 (m), 1123 (m), 807 (m), 756 (m), 696 (m), 651 (m), 505 (w). ^1H NMR

(300 MHz, $CDCl_3$) δ: 10.05 (s, 1H), 8.86–8.85 (d, J=1.5 Hz, 1H), 8.44 (s, 1H), 8.24–8.21 (d, J=7.8 Hz, 1H), 8.08–8.04 (dd, J=8.7 Hz, 1.8 Hz, 1H), 8.68–8.34 (m, 9H). ^{13}C NMR (75 MHz, $CDCl_3$) δ: 181.9, 176.8, 152.6, 142.8, 141.6, 137.8, 136.8, 130.0, 128.1, 127.0, 126.9, 125.4, 124.7, 123.8, 123.0, 120.9, 120.7, 119.8, 110.3. EI–TOF–MS (m/z): calcd for $[C_{22}H_{14}N_2OS]^+$ 354.1 (100%), 355.1 (24.0%), 356.1 (4.7%), found 354.1 (100%), 355.1 (5.8%), 356.1 (0.4%). Anal. Calcd for $C_{22}H_{14}N_2OS$: C, 74.55, H, 3.98, N, 7.90%. Found: C, 74.41, H, 3.83, N, 8.07%.

4.2.4. Compound **7**. $TiCl_4$ (0.62 mL, 5.63 mmol) dissolved in anhydrous dichloromethane (10 mL) was carefully added into dry THF (30 mL) at 0 °C.[23] Zinc dust (0.73 g, 11.3 mmol) was added and then the mixture was refluxed at 85 °C for 2 h. Pyridine (0.48 mL, 5.63 mmol) was added and the mixture was refluxed for another 1 h. After cooling to ambient temperature, a solution of compound **1** (0.40 g, 1.13 mmol) in dry THF (20 mL) was added and the reaction mixture was refluxed at 85 °C for 2 days. The reaction was quenched with water at 0 °C, then the mixture was extracted with $CHCl_3$ (3×40 mL) and washed with saturated NH_4Cl (50 mL) and H_2O (3×40 mL), and then dried over anhydrous $MgSO_4$. After removing the solvent in vacuo, the crude product was purified by column chromatography on silica gel with petroleum ether (60–90 °C) and dichloromethane (v/v=2:1) as eluent to produce 0.20 g (52%) compound **7** as orange solid. Mp: 213–215 °C. Main FTIR absorptions (KBr pellets, cm^{-1}): 3450 (m), 1586 (s), 1486 (s), 1321 (m), 1274 (s), 1180 (w), 933 (w), 830 (w), 795 (m), 754 (m), 693 (m), 511 (m). ^{1}H NMR (300 MHz, $CDCl_3$) δ: 7.48–7.44 (dt, J=8.7 Hz, 2.7 Hz, 4H), 7.30–7.28 (m, 6H), 7.25 (s, 2H), 7.14–7.11 (m, 10H), 7.08–7.02 (m, 8H), 6.99–6.97 (m, 4H). ^{13}C NMR (75 MHz, $CDCl_3$) δ: 147.3, 142.8, 141.0, 129.2, 128.1, 127.3, 126.3, 124.5, 123.4, 123.1, 122.6, 121.0. EI–TOF–MS (m/z): calcd for $[C_{46}H_{34}N_2S_2]^+$ 678.2 (100%), 679.2 (51.7%), 680.2 (13.3%), found 677.9 (100%), 679.1 (68.7%), 680.0 (6.7%). Anal. Calcd for $C_{46}H_{34}N_2S_2$: C, 81.38, H, 5.05, N, 4.13%. Found: C, 81.23, H, 5.11, N, 4.08%.

4.2.5. Compound **8**. Synthesis of this compound was similar to that described for compound **7** except that compound **2** (0.40 g, 1.13 mmol) was used instead of compound **1**. Compound **8** was obtained as pale yellow powder in a yield of 0.18 g (47%) after column chromatography of the crude product on silica gel with petroleum ether/CH_2Cl_2 (v/v=2:1) as eluent. Mp: 211–213 °C. Main FTIR absorptions (KBr pellets, cm^{-1}): 3426 (m), 2918 (s), 2850 (m), 1601 (m), 1513 (s), 1450 (s), 1326 (m), 1229 (m), 1110 (m), 802 (m), 750 (s), 723 (m), 505 (m). ^{1}H NMR (300 MHz, $CDCl_3$) δ: 8.22–8.16 (dd, J=12.3 Hz, 7.8 Hz, 8H), 7.89 (s, 2H), 7.73–7.70 (d, J=8.7 Hz, 4H), 7.52–7.30 (m, 14H), 7.14 (s, 2H). ^{13}C NMR (75 MHz, $CDCl_3$) δ: 166.6, 149.7, 146.9, 142.7, 136.2, 129.4, 127.4, 126.6, 125.2, 123.8, 121.9, 120.6. EI–TOF–MS (m/z): calcd for $[C_{46}H_{30}N_2S_2]^+$ 674.2 (100%), 675.2 (50.1%), 676.2 (13.5%), found 674.2 (100%), 675.3 (76.9%), 676.3 (6.6%). Anal. Calcd for $C_{46}H_{30}N_2S_2$: C, 81.87, H, 4.48, N, 4.15%. Found: C, 81.78, H, 4.63, N, 4.20%.

4.2.6. Compounds ***10*** *and* ***4a***. The procedure for preparing compound **7** was repeated except that thiazole based aldehyde **4** (0.40 g, 1.13 mmol) was used instead of thiophene based aldehyde **1**. Compound **4a** was obtained as a by-product of this reaction. Compounds **10** and **4a** were purified by silica gel column chromatography of the crude product using hexane and dichloromethane (v/v=1:2) as eluent to give **10** as orange solid and **4a** as colorless solid in the yields of 0.17 g (45%) and 0.04 g (10%), respectively. Compound **10**: Mp: 210–212 °C. Main FTIR absorptions (KBr pellets, cm^{-1}): 3439 (m), 1587 (s), 1492 (s), 1439 (m), 1410 (m), 1323 (m), 1281 (s), 1180 (w), 1146 (w), 834 (w), 755 (w), 696 (m), 629 (w), 588 (w), 515 (w). ^{1}H NMR (300 MHz, $CDCl_3$) δ: 7.79–7.76 (dt, J=8.7 Hz, 1.8 Hz, 8H), 7.70 (s, 2H), 7.33–7.28 (m, 8H), 7.16–7.06 (m, 16H), 6.97 (s, 2H). ^{13}C NMR (75 MHz, $CDCl_3$) δ: 143.7, 140.7, 136.4, 133.6, 127.3, 126.8, 126.7, 126.0, 125.9, 123.3, 123.2, 120.2, 120.0, 109.7. EI–TOF–MS (m/z): calcd for $[C_{44}H_{32}N_4S_2]^+$ 680.2 (100%), 681.2 (49.6%), 682.2 (12.5%), found 680.2 (100%), 681.2 (23.2%), 682.2 (1.9%). Anal. Calcd for $C_{44}H_{32}N_4S_2$: C, 77.62, H, 4.74, N, 8.23%. Found: C, 77.51, H, 4.98, N, 8.34%. Compound **4a**: Mp: 177–180 °C. Main FTIR absorptions (KBr pellets, cm^{-1}): 3429 (m), 2923 (w), 1589 (s), 1489 (m), 1444 (m), 1323 (s), 1277 (s), 1108 (m), 847 (w), 815 (w), 755 (m), 696 (s), 630 (w), 505 (m). ^{1}H NMR (300 MHz, $CDCl_3$) δ: 7.75–7.70 (d, J=8.7 Hz, 2H), 7.44 (d, J=1.2 Hz, 1H), 7.31–7.25 (m, 4H), 7.14–7.04 (m, 8H), 2.48 (s, 3H). EI–TOF–MS (m/z): calcd for $[C_{22}H_{18}N_2S]^+$ 342.1 (100%), 343.1 (25.3%), 344.1 (4.5%), found 342.2 (100%), 343.2 (11.9%), 344.2 (1.1%). Anal. Calcd for $C_{22}H_{18}N_2S$: C, 77.16, H, 5.30, N, 8.18%. Found: C, 77.07, H, 5.23, N, 8.23%.

4.2.7. Compound ***11***. The synthetic procedure of compound **11** was the same as that of compound **7** except that aldehyde **5** (0.40 g, 1.13 mmol) was used instead of aldehyde **1**. Compound **11** was obtained as light yellow solid in a yield of 0.12 g (31%) after column chromatography of the crude product on silica gel with hexane/DCM (v/v=1:2) as eluent. Mp: 211–213 °C. Main FTIR absorptions (KBr pellets, cm^{-1}): 3452 (m), 2960 (m), 2853 (m), 1715 (w), 1597 (m), 1514 (m), 1444 (s), 1341 (m), 1261 (s), 1223 (w), 1097 (s), 1024 (s), 805 (s), 743 (m), 629 (w). ^{1}H NMR (300 MHz, $CDCl_3$) δ: 8.22–8.16 (dd, J=12.3 Hz, 7.8 Hz, 8H), 7.89 (s, 2H), 7.73–7.70 (d, J=8.7 Hz, 4H), 7.52–7.31 (m, 14H), 7.14 (s, 2H). EI–TOF–MS (m/z): calcd for $[C_{44}H_{28}N_4S_2]^+$ 676.2 (100%), 677.2 (47.9%), 344.1 (12.5%), found 676.1 (100%), 677.1 (59.4%), 344.2 (7.4%). Anal. Calcd for $C_{44}H_{28}N_4S_2$: C, 78.08, H, 4.17, N, 8.28%. Found: C, 78.19, H, 4.35, N, 8.39%.

Acknowledgements

This work was financially supported by the Major State Basic Research Development Programs (Nos. 2013CB922101 and 2011CB933300), the National Natural Science Foundation of China (No. 21171088), and the Natural Science Foundation of Jiangsu Province (Nos. BK20130054 and BE2014147-1).

Supplementary data

Supplementary data (FTIR, EI–TOF–MS, ^{1}H and ^{13}C NMR spectra, TGA diagrams, HOMOs/LUMOs and temperature-dependent I–V curves for related compounds. CCDC numbers 1052650–1052654 contain the supplementary crystallographic data for this paper. These data can be obtained free of charge at www.ccdc.cam.ac.uk/conts/retrieving.html [or from the Cambridge Crystallographic Data Centre, 12, Union Road, Cambridge CB2 1EZ, UK; Fax: (internat.) +44-1223/336-033; E-mail: deposit@ccdc.cam.ac.uk].) related to this article can be found at http://dx.doi.org/10.1016/j.tet.2015.04.045.

References and notes

1. (a) Roncali, J. *Chem. Rev.* **1997**, *97*, 173–205; (b) Martin, R. E.; Diederich, F. *Angew. Chem., Int. Ed.* **1999**, *38*, 1350–1377; (c) Newman, C. R.; Gerlach, C. P.; Kelley, T. W.; Muyres, D. V.; Fritz, S. E.; Toney, M. F.; Frisbie, C. D. *J. Am. Chem. Soc.* **2005**, *127*, 3997–4009; (d) Bazan, G. C. *J. Org. Chem.* **2007**, *72*, 8615–8635; (e) Wang, C.-L.; Dong, H.-L.; Hu, W.-P.; Liu, Y.-Q.; Zhu, D.-B. *Chem. Rev.* **2012**, *112*, 2208–2267.
2. (a) Zhong, C. M.; Duan, C. H.; Huang, F.; Wu, H. B.; Cao, Y. *Chem. Mater.* **2011**, *23*, 326–340; (b) Tao, Y. T.; Yang, C. L.; Qin, J. L. *Chem. Soc. Rev.* **2011**, *40*, 2943–2970; (c) Greiner, M. T.; Helander, M. G.; Tang, W.-M.; Wang, Z.-B.; Qiu, J.; Lu, Z.-H. *Nat. Mater.* **2012**, *11*, 76–81.
3. (a) Hains, A. W.; Liang, Z. Q.; Woodhouse, M. A.; Gregg, B. A. *Chem. Rev.* **2010**, *110*, 6689–6735; (b) Lin, Y. Z.; Li, Y. F.; Zhan, X. W. *Chem. Soc. Rev.* **2012**, *41*, 4245–4272; (c) Yella, A.; Lee, H. W.; Tsao, H. N.; Yi, C. Y.; Chandiran, A. K.; Nazeeruddin, M. K.; Diau, E. W. G.; Yeh, C. Y.; Zakeeruddin, S. M.; Gratzel, M.

Science **2011**, *334*, 629–634; (d) Li, G.; Zhu, R.; Yang, Y. *Nat. Photonics* **2012**, *6*, 153–161.
4. (a) Klauk, H. *Chem. Soc. Rev.* **2010**, *39*, 2643–2666; (b) Mei, J. G.; Diao, Y.; Appleton, A. L.; Fang, L.; Bao, Z. N. *J. Am. Chem. Soc.* **2013**, *135*, 6724–6746; (c) Wu, W. P.; Liu, Y. Q.; Zhu, D. B. *Chem. Soc. Rev.* **2010**, *39*, 1489–1502; (d) Shinamura, S.; Osaka, I.; Miyazaki, E.; Nakao, A.; Yamagishi, M.; Takeya, J.; Takimiya, K. *J. Am. Chem. Soc.* **2011**, *133*, 5024–5035; (e) Liu, Z. T.; Zhang, G. X.; Cai, Z. X.; Chen, X.; Luo, H. W.; Li, Y. H.; Wang, J. G.; Zhang, D. Q. *Adv. Mater.* **2014**, *26*, 6965–6977; (f) Gao, X. K.; Hu, Y. B. *J. Mater. Chem. C* **2014**, *2*, 3099–3117; (g) Lin, Y. Z.; Fan, H. J.; Li, Y. F.; Zhan, X. W. *Adv. Mater.* **2012**, *24*, 3087–3106.
5. (a) Collis, G. E.; Burrell, A. K.; Scott, S. M.; Officer, D. L. *J. Org. Chem.* **2003**, *68*, 8974–8983; (b) Grant, D. K.; Jolley, K. W.; Officer, D. L.; Gordon, K. C.; Clarke, T. M. *Org. Biomol. Chem.* **2005**, *3*, 2008–2015; (c) Roncali, J. *J. Mater. Chem.* **1999**, *9*, 1875–1893; (d) Roncali, J. *Ann. Rep. Prog. Chem., Sect. C* **1999**, *95*, 47–88.
6. (a) Rajca, A.; Wang, H.; Pink, M.; Rajca, S. *Angew. Chem., Int. Ed.* **2000**, *39*, 4481–4483; (b) Miyasaka, M.; Rajca, A.; Pink, M.; Rajca, S. *J. Am. Chem. Soc.* **2005**, *127*, 13806–13807; (c) Miyasaka, M.; Rajca, A. *J. Org. Chem.* **2006**, *71*, 3264–3266.
7. Sun, Y. M.; Tan, L.; Jiang, S. D.; Qian, H. L.; Wang, Z. H.; Yan, D. W.; Di, C. A.; Wang, Y.; Wu, W. P.; Yu, G.; Yan, S. K.; Wang, C. R.; Hu, W. P.; Liu, Y. Q.; Zhu, D. B. *J. Am. Chem. Soc.* **2007**, *129*, 1882–1883.
8. (a) Anthony, J. E.; Brooks, J. S.; Eaton, D. L.; Parkin, S. R. *J. Am. Chem. Soc.* **2001**, *123*, 9482–9483; (b) Curtis, M. D.; Gao, J.; Kampf, J. W. *J. Am. Chem. Soc.* **2004**, *126*, 4318–4328; (c) Bredas, J.-L.; Deljonne, D.; Coropceanu, V.; Cornil, J. *Chem. Rev.* **2004**, *104*, 4971–5003; (d) Sirringhaus, H.; Brown, P. J.; Friend, R. H.; Nielsen, M. M.; Bechgaard, K.; Langeveld-Voss, B. M. W.; Spiering, A. J. H.; Janssen, R. A. J.; Meijer, E. W.; Herwig, P.; de Leeuw, D. M. *Nature* **1999**, *401*, 685–688.
9. Rao, V. P.; Cai, Y. M.; Jen, K. Y. *Chem. Commun.* **1994**, 1689–1690.
10. Elandaloussi, P.; Frère, P.; Richomme, P.; Orduna, J.; Garin, J.; Roncali, J. *J. Am. Chem. Soc.* **1997**, *119*, 10774–10784.
11. Jestin, I.; Frère, P.; Mercier, N.; Levillain, E.; Stievenaed, D.; Roncali, J. *J. Am. Chem. Soc.* **1998**, *120*, 8150–8158.
12. (a) Blohm, M. L.; Pickett, J. E.; Van Dort, P. C. *Macromolecules* **1993**, *26*, 2704–2710; (b) Catellani, M.; Luzzati, S.; Musco, A.; Speroni, F. *Synth. Met.* **1994**, *62*, 223–228; (c) Eckhardt, H.; Shacklette, L. W.; Jen, K. Y.; Elsenbaumer, R. L. *J. Chem. Phys.* **1989**, *91*, 1303–1315; (d) Geisler, T.; Petersen, J. C.; Bjornholm, T.; Fisher, E.; Larsen, J.; Dehu, C.; Bredas, J. L.; Tormos, G. V.; Nugara, P. N.; Cava, M. P.; Meyzger, R. M. *J. Phys. Chem.* **1994**, *98*, 10102–10111.
13. (a) Xue, C. H.; Luo, F. T. *Tetrahedron* **2003**, *59*, 5193–5198; (b) Hou, J. H.; Tan, Z. A.; He, Y. J.; Yang, C. H.; Li, Y. F. *Macromolecules* **2006**, *39*, 4657–4662; (c) Zhang, L.; Tan, L.; Hu, W. P.; Wang, Z. H. *J. Mater. Chem.* **2009**, *19*, 8216–8222; (d) Tan, L.; Zhang, L.; Jiang, X.; Yang, X. D.; Wang, L. J.; Wang, Z. H.; Li, L. Q.; Hu, W. P.; Shuai, Z. G.; Li, L.; Zhu, D. B. *Adv. Funct. Mater.* **2009**, *19*, 272–276.
14. (a) Tao, T.; Qian, H. F.; Zhang, K.; Geng, J.; Huang, W. *Tetrahedron* **2013**, *69*, 7290–7299; (b) Tao, T.; Ma, B. B.; Peng, Y. X.; Wang, X. X.; Huang, W.; You, X. Z. *J. Org. Chem.* **2013**, *78*, 8669–8679; (c) Tao, T.; Peng, Y. X.; Huang, W.; You, X. Z. *J. Org. Chem.* **2013**, *78*, 2472–2481.
15. (a) Bolduc, A.; Ouahabi, A. A.; Mallet, C.; Skene, W. G. *J. Org. Chem.* **2013**, *78*, 9258–9269; (b) Frère, P.; Raimundo, J.; Blanchard, P.; Delaunay, J.; Richomme, P.; Sauvajol, J.; Orduna, J.; Garin, J.; Roncali, J. *J. Org. Chem.* **2003**, *68*, 7254–7265; (c) Hu, Y.; Wex, B.; Perkovic, M. W.; Neckers, D. C. *Tetrahedron* **2008**, *64*, 2251–2258; (d) Wang, J.-L.; Zhong, C. M.; Tang, Z.-M.; Wu, H. B.; Ma, Y. G.; Cao, Y.; Pei, J. *Chem.—Asian J.* **2010**, *5*, 105–113.
16. (a) Johansson, T.; Mammo, W.; Svensson, M.; Andersson, M. R.; Ingans, O. *J. Mater. Chem.* **2003**, *13*, 1316–1323; (b) Ma, C. Q.; Pisula, W.; Weber, C.; Feng, X. L.; Mullen, K.; Bauerle, P. *Chem.—Eur. J.* **2011**, *17*, 1507–1518.
17. (a) Araki, K.; Endo, H.; Masuda, G.; Ogawa, T. *Chem.—Eur. J.* **2004**, *10*, 3331–3340; (b) Huang, W.; Masuda, G.; Maeda, S.; Tanaka, H.; Ogawa, T. *Chem.—Eur. J.* **2006**, *12*, 607–619; (c) Huang, W.; Tanaka, H.; Ogawa, T. *J. Phys. Chem. C* **2008**, *112*, 11513–11526; (d) Tao, T.; Geng, J.; Hong, L.; Huang, W.; Tanaka, H.; Tanaka, D.; Ogawa, T. *J. Phys. Chem. C* **2013**, *117*, 25325–25333; (e) Ammann, M.; Bäuerle, P. *Org. Biomol. Chem.* **2005**, *3*, 4143–4152.
18. (a) Cai, S. Y.; Hu, X. H.; Zhang, Z. Y.; Su, J. H.; Li, X.; Islam, A.; Han, L. Y.; Tian, H. *J. Mater. Chem. A* **2013**, *1*, 4763–4772; (b) Liu, W.-H.; Wu, I.-C.; Lai, C.-H.; Lai, C.-H.; Chou, P.-T.; Li, Y.-T.; Chen, C.-L.; Hsu, Y.-Y.; Chi, Y. *Chem. Commun.* **2008**, 5152–5154; (c) Sakong, C.; Kim, S. H.; Yuk, S. B.; Namgoong, J. W.; Park, S. W.; Ko, M. J.; Kim, D. H.; Hong, K. S.; Kim, J. P. *Chem.—Asian J.* **2012**, *8*, 1817–1826.
19. Kubin, R. F.; Fletcher, A. N. *J. Lumin.* **1983**, *27*, 455–462.
20. Frisch, M. J.; Trucks, G. W.; Schlegel, H. B.; Scuseria, G. E.; Robb, M. A.; Cheeseman, J. R.; Scalmani, G.; Barone, V.; Mennucci, B.; Petersson, G. A.; Nakatsuji, H.; Caricato, M.; Li, X.; Hratchian, H. P.; Izmaylov, A. F.; Bloino, J.; Zheng, G.; Sonnenberg, J. L.; Hada, M.; Ehara, M.; Toyota, K.; Fukuda, R.; Hasegawa, J.; Ishida, M.; Nakajima, T.; Honda, Y.; Kitao, O.; Nakai, H.; Vreven, T.; Montgomery, J. A., Jr.; Peralta, J. E.; Ogliaro, F.; Bearpark, M.; Heyd, J. J.; Brothers, E.; Kudin, K. N.; Staroverov, V. N.; Keith, T.; Kobayashi, R.; Normand, J.; Raghavachari, K.; Rendell, A.; Burant, J. C.; Iyengar, S. S.; Tomasi, J.; Cossi, M.; Rega, N.; Millam, J. M.; Klene, M.; Knox, J. E.; Cross, J. B.; Bakken, V.; Adamo, C.; Jaramillo, J.; Gomperts, R.; Stratmann, R. E.; Yazyev, O.; Austin, A. J.; Cammi, R.; Pomelli, C.; Ochterski, J. W.; Martin, R. L.; Morokuma, K.; Zakrzewski, V. G.; Voth, G. A.; Salvador, P.; Dannenberg, J. J.; Dapprich, S.; Daniels, A. D.; Farkas, O.; Foresman, J. B.; Ortiz, J. V.; Cioslowski, J.; Fox, D. J. *Gaussian 09, Revision C.01*; Gaussian: Wallingford, CT, 2010.
21. SMART and SAINT, Area Detector Control and Integration Software; Siemens Analytical X-ray Systems: Madison, WI, 2000.
22. Sheldrick, G. M. *SHELXTL (Version 6.10). Software Reference Manual*; Bruker AXS: Madison, Wisconsin (USA), 2000.
23. (a) McMurry, J. E.; Fleming, M. P.; Kees, K. L.; Krepski, L. R. *J. Org. Chem.* **1978**, *43*, 3255–3266; (b) Iyoda, M.; Huang, P.; Nishiuchi, T.; Takase, M.; Nishinaga, T. *Heterocycles* **2011**, *82*, 1143–1149; (c) Wu, T. J.; Shi, J. W.; Li, C. L.; Song, J. S.; Xu, L.; Wang, H. *Org. Lett.* **2013**, *15*, 354–357.

Please cite this article in press as: Xi, B.; et al., Tetrahedron (2015), http://dx.doi.org/10.1016/j.tet.2015.04.045